Experimental evaluation of a new class of algorithms for active noise attenuation

Ioan Doré Landau, Tudor-Bogdan Airimitoaie, Raúl Antonio Meléndez, Gabriel Buche, Luc Dugard

Experimental evaluation of a new class of algorithms for active noise attenuation

Ioan Doré Landau[1], Tudor-Bogdan Airimitoaie[2], Raul Melendez[1], Gabriel Buche[1], and Luc Dugard[1]

[1]Univ. Grenoble Alpes, CNRS, Grenoble INP, GIPSA-lab, 38000 Grenoble, France
[2]Univ. Bordeaux, Bordeaux INP, CNRS, IMS, 33405 Talence, France

Abstract: Historically adaptive feedforward noise compensation using the so called LMS adaptation algorithm has been considered as the basic solution for active noise attenuation despite a number of drawbacks. In fact one can reject unknown and time-varying multiple narrow-band noises without requiring information upon the noise using an adaptive feedback active attenuation scheme. The implementation of this type of scheme uses the Internal Model Principle and the Youla–Kučera parametrization as well as improved adaptation algorithms. For attenuation of broad-band noise, while one still uses a feedforward compensation scheme, new adaptation algorithms have been developed which take into account the interaction between the measurement of the incoming noise and the operation of the compensation device (leading to an internal positive feedback loop which may cause instability). The use of the Youla–Kučera parametrization allows to separate the problem of the stability of the internal positive feedback loop from the problem of optimization of the parameters of the feedforward compensator. This allows also to go beyond the limitations of the length of the compensation path. Experimental results are presented in the last part of the paper.

Keywords: active noise control, adaptive feedforward compensation, Youla–Kučera parametrization, positive feedback coupling.

1 Introduction

Adaptive feedforward noise attenuation is widely used when a well correlated signal with the disturbance (image of the disturbance) is available ([3, 6, 17]). The first references go back roughly to 1985 ([16]). In most of the systems, there is a positive acoustic coupling between the feedforward compensation system and the measurement of the image of the disturbance. This often leads to the instability of the system. In the context of this inherent "positive" feedback, the adaptive feedforward compensator should minimize the effect of the disturbance while simultaneously assuring the stability of the internal positive feedback loop. This problem has been clearly identified by the mid nineties [6, 5].
Figure 1 gives the basic block diagram of the adaptive feedforward compensation in the presence of the internal positive coupling between the output of the compensator and the measurement of the image of the incoming noise. The incoming noise propagates through the so called *primary path* T and its effect is compensated by a secondary noise source through the *secondary path* G driven by a feedforward compensator $\hat{N}$. The input to the feedforward compensator is the sum of the image of the incoming noise and of the internal acoustical positive feedback through M. The residual noise is used to emulate the adaptation of the feedforward compensator.

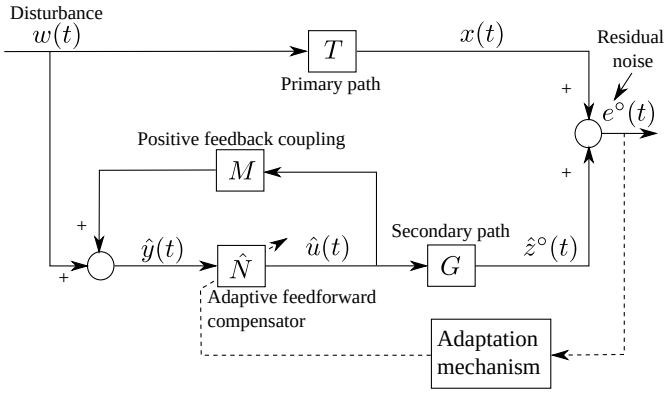

Figure 1: Feedforward AVC with adaptive feedforward compensator.

A major component of such a system is the PAA (parameter adaptation algorithm). In the field of ANC (active noise control), the first algorithm used was the so called LMS (least mean squares, see[16]) derived from a local minimization of a quadratic criterion in terms of the residual noise. Many contributions have been done on the analysis of the properties of this algorithm[1] and the improvement of the algorithm. Filtering of the regressor vector was one of the ways for improving the adaptation algorithm. The FULMS algorithm [4][2] which seems to be the most used algorithm in adaptive feedforward compensation can be viewed as a particular approximation of the algorithms derived from stability considerations in [14].

[1]However these attempts have not solved the stability problem in the presence of the internal "positive" feedback.

[2]It is used with an IIR structure of the feedforward compensator. When it is used with a FIR feedforward compensator it is denoted FXLMS.

A major step forward in the design of the adaptive feedforward compensators in the presence of the internal positive feedback coupling was the introduction of the Youla–Kučera parametrization allowing to separate the stabilization of the internal positive feedback loop from the optimization of the parameters of the feedforward compensator. This ideea has been prompted out for the first time in [17]. A full synthesis procedure has been presented in [12, 7]. Examples of applications in active noise control can be found in [10, 9].
At the end of the nineties, adaptive feedback noise control emerged as an efficient solution for cancelling single or multiple tonal disturbances ([1]), ([2]) taking advantage of the internal model principle and the Youla–Kučera parametrization of the feedback controller. Fig. 2 gives the block diagram of such a system.

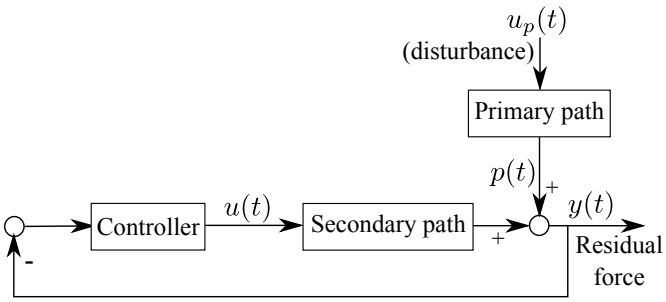

Figure 2: Adaptive feedback noise attenuation.

The feedback approach is mainly dedicated to the attenuation of unknown time-varying multiple narrow-band noises while the feedforward approach is dedicated for the attenuation of broad-band noise with unknown and time-varying characteristics.

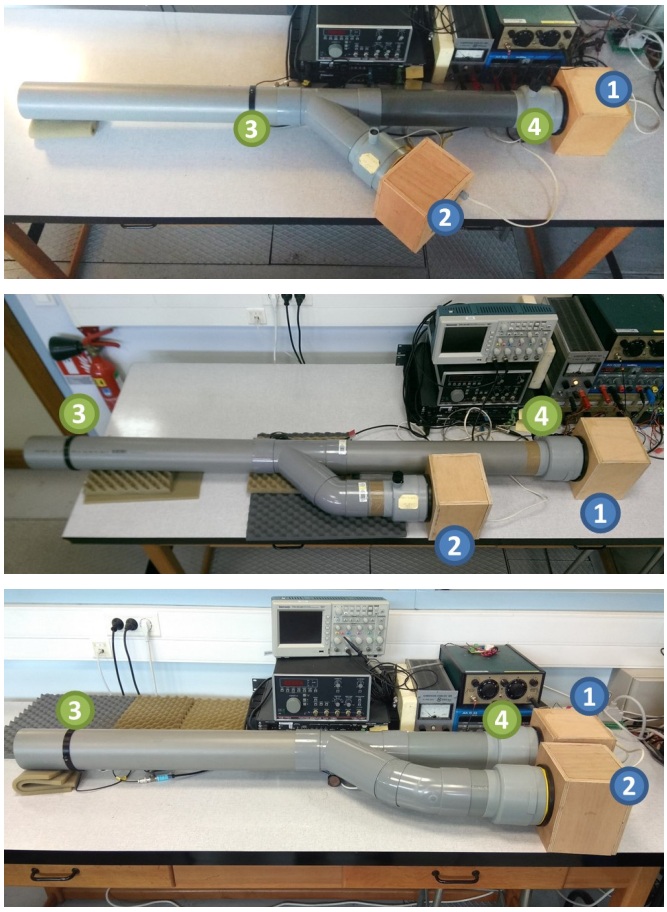

Figure 3: Duct active noise control test bench-Configuration (Photo): configuration V1 (top), configuration V2 (middle), configuration V3 (bottom)

2 Experimental Setup

The views of the various configurations of the test-bench used for experiments are shown in Fig. 3 and its detailed scheme is given in Fig. 4.
The speaker used as the source of disturbances is labelled as 1, while the control speaker is marked as 2. At pipe's open end, the microphone that measures the system's output (residual noise $e(t)$) is denoted as 3. Inside the pipe, close to the source of disturbances, the second microphone, labelled as 4, measures the perturbations' image, denoted as $y(t)$. Additionally, we denote $u(t)$ the control signal, and $s(t)$ the disturbance. The transfer function between the disturbance's speaker and the microphone (1→3) is called *Global Primary Path*, while the transfer function between the control speaker and the microphone (2→3) is denoted *Secondary Path*. The transfer function between microphones (4→3) is called *Primary Path*. The internal coupling found between (2→4) is denoted *Reverse Path*. These marked paths have a double differentiator behaviour, since as input we have the voice coil displacement and as output the air acoustic pressure. For the feedback attenuation configuration the microphone 4 is unnecessary. The speakers

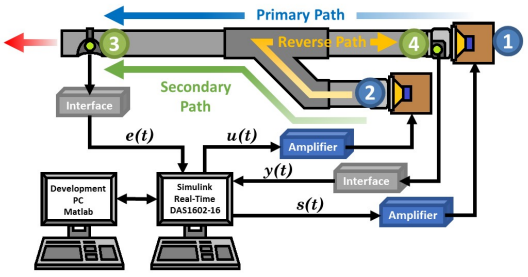

Figure 4: Duct active noise control test-bench diagram.

are isolated inside wood boxes filled with special foam in order to create anechoic chambers and reduce the radiation noise produced.
Both speakers are connected to a xPC Target computer with Simulink Real-time® environment through a pair of high definition power amplifiers and a data acquisition board. A second computer is used for development, design and operation with Matlab®. The sampling frequency has been chosen in accordance with the recommendations given in

[13]. Taking into account that disturbances up to 400 Hz may need to be attenuated, a sampling frequency $f_s = 2500$ Hz has been chosen ($T_s = 0.0004$ sec), i.e., approximately six times the maximum frequency to attenuate.

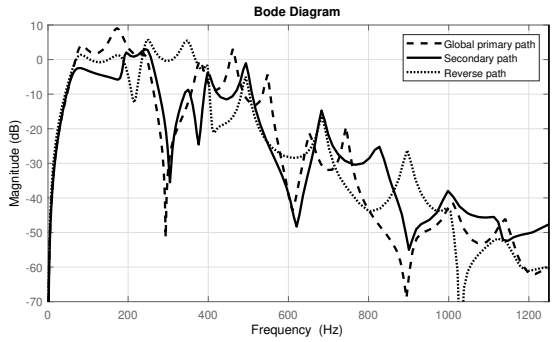

Figure 5: Frequency characteristics of the Primary, Secondary and Reverse paths identified models.

The frequency characteristics of the identified models for the primary[3], secondary and reverse [4] paths are shown in Fig. 5 for the version V1 of the test-bench. These characteristics present multiple resonances (low damped complex poles) and anti-resonances (low damped complex zeros). For the other configurations while the location of the resonances and anti-resonances will be different the general feature will be similar.

It is important to note that most of the implementations of the adaptive feedforward compensation systems are close to a co-location of the residual noise measurement and of the secondary source used for compensation. A ratio of 1/6 to 2/6 between the length of the secondary path and the length of the primary path is generally used. Nevertheless, there are new potential applications areas (exhaust noise reduction on boats, trucks, cars) where thermal constraints will not allow to have a configuration close to a co-location. For this reason the ratio between the length of the secondary path and the length of the primary path has been chosen about 5/6 (close to the theoretical limit) as well beyond (7/6) for the version V3 (see Fig. 3).

3 Adaptive feedforward noise attenuation

Figure 1 gives the basic structures of the adaptive feedforward attenuation schemes where the feedforward compensator can have a FIR or an IIR structure. The compensator N has the form $N = \frac{R}{S}$. The estimated polynomials R and S will be denoted $\hat{R}(q^{-1})$ and $\hat{S}(q^{-1})$ (for $S = 1$ one has a FIR compensator).

The corresponding block diagram for the adaptive feedforward compensation using IIR Youla–Kučera parametrization of the feedforward compensator is shown in Fig. 6. $\hat{y}(t)$ denotes the effective output provided by the measurement device and which will serve as input to the adaptive feedforward filter $\hat{N}$. in this case the adaptive feeforward compensator is formed by the central controller R_0/S_0 and the adjustable estimated filter $\hat{B}_Q/\hat{A}_Q$. The output of this filter denoted by $\hat{u}(t)$ is applied to the actuator through an amplifier.

For $A_Q = 1$ one gets an FIR Youla–Kučera parametrization. In this case the poles of the internal positive feedback loop will be defined by the choice of S_0 and R_0 and will remain unchanged independently of the values of the parameters of the estimated polynomial $\hat{B}_Q$. Details can be found in [12, 7].

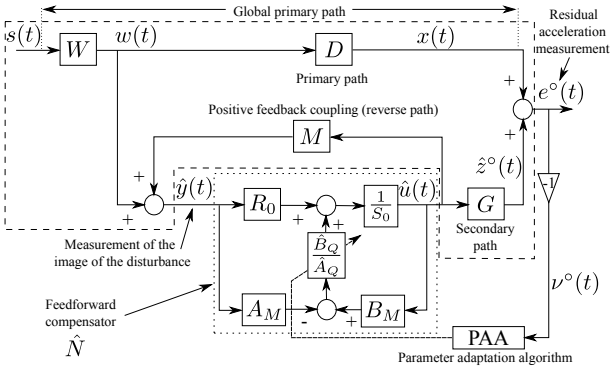

Figure 6: Feedforward ANVC with IIRYK adaptive feedforward compensator.

4 Adaptive feedback noise attenuation

The adaptive feedback noise attenuation configuration using the Youla–Kučera parametrization is shown in Fig. 7 where $S_0(q^{-1})$ and $R_0(q^{-1})$ define the central controller.

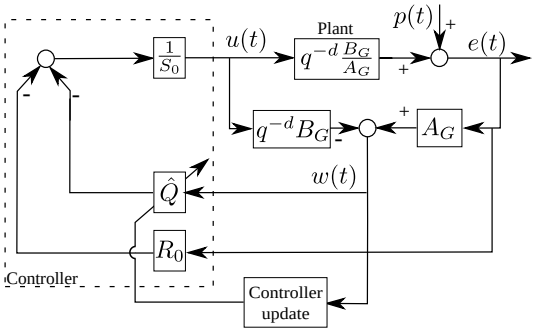

Figure 7: Direct adaptive feedback scheme for rejection of unknown disturbances.

The characteristic polynomial, which specifies the desired

[3] The primary path model has been exclusively used for simulation purposes.

[4] In the feedback approach this path is not used since there is no a second microphone

closed loop poles of the system is given by (see also [11]):[5]

$$P_0(z^{-1}) = A_G(z^{-1})S_0(z^{-1}) + z^{-d}B_G(z^{-1})R_0(z^{-1}). \quad (1)$$

When the Youla–Kučera parametrization is used with a FIR Q polynomial the poles of the closed loop defined by (1) remain unchanged independently of the values of the parameters of the Q filter. In this case the controller's polynomials become:

$$R = R_0 + A_G Q, \quad (2)$$

$$S = S_0 - z^{-d}B_G Q, \quad (3)$$

A key aspect of this methodology is the use of the Internal Model Principle (IMP). It is supposed that $p(t)$ is a deterministic disturbance given by

$$p(t) = \frac{N_p(q^{-1})}{D_p(q^{-1})} \cdot \delta(t), \quad (4)$$

where $\delta(t)$ is a Dirac impulse and N_p, D_p are coprime polynomials of degrees n_{N_p} and n_{D_p}, respectively[6]. In the case of stationary narrow-band disturbances, the roots of $D_p(z^{-1})$ are on the unit circle.

Internal Model Principle [8]: The effect of the disturbance given in (4) upon the output is given by

$$e(t) = \frac{A_G(q^{-1})S(q^{-1})}{P(q^{-1})} \cdot \frac{N_p(q^{-1})}{D_p(q^{-1})} \cdot \delta(t), \quad (5)$$

where $D_p(z^{-1})$ is a polynomial with roots on the unit circle and $P(z^{-1})$ is an asymptotically stable polynomial. $y(t)$ in Eq. (5) converges asymptotically towards zero if and only if the polynomial $S(z^{-1})$ in the (equivalent) RS controller has the form:

$$S(z^{-1}) = D_p(z^{-1})S'(z^{-1}). \quad (6)$$

One can see that the polynomial S of the controller incorporates in this case the denominator of the model of the disturbance. It turns out that using the Youla–Kučera parametrization the introduction of the internal model of the disturbance in the controller in the presence of unknown disturbances can be achieved by the direct adaptation of the parameters of the Q polynomial. Details can be found in [15].

5 Parameter Adaptation Algorithms

The PAA used in all the schemes has the general form:

$$\hat{\theta}(t+1) = \hat{\theta}(t) + F(t)\psi(t)\nu(t+1)\ ; \quad (7)$$

$$\nu(t+1) = \frac{\nu^\circ(t+1)}{1+\psi^T(t)F(t)\psi(t)}\ ; \quad (8)$$

$$F(t+1) = \frac{1}{\lambda_1(t)}\left[F(t) - \frac{F(t)\psi(t)\psi^T(t)F(t)}{\frac{\lambda_1(t)}{\lambda_2(t)} + \psi^T(t)F(t)\psi(t)}\right] \quad (9)$$

$$1 \geq \lambda_1(t) > 0; 0 \leq \lambda_2(t) < 2; F(0) > 0 \quad (10)$$

$$\psi(t) = \phi_f(t) = L(q^{-1})\phi(t), \quad (11)$$

where $\lambda_1(t)$ and $\lambda_2(t)$ allow to obtain various time profiles for the matrix adaptation gain $F(t)$ (see [8]). By taking $\lambda_2(t) \equiv 0$ and $\lambda_1(t) \equiv 1$, one gets a constant adaptation gain matrix.

$$\hat{\theta}(t+1) = \hat{\theta}(t) + F(t)\psi(t)\frac{\nu^\circ(t+1)}{1+\psi^T(t)F(t)\psi(t)} \quad (12)$$

$$\nu^\circ(t) = -e^\circ(t) \quad (13)$$

Two types of adaptation gain allowing to operate in an "adaptive" regime are mostly used:

- *Constant trace algorithm*. $\lambda_1(t)$ and $\lambda_2(t)$ are adjusted continuously to maintain constant the trace of the adaptation gain matrix. This allows to move in the optimal direction while maintaining the adaptation capabilities.
- *Constant scalar adaptation gain*. This is obtained by taking $\lambda_1(t) \equiv 1$, $\lambda_2(t) \equiv 0$ and $F(t) = \gamma I, \gamma > 0$ where I is the identity matrix.

The values of $\lambda_1(t)$ and $\lambda_2(t)$ in order to maintain constant the trace of the adaptation gain matrix are determined from the equation:

$$tr\left(F(t+1)\right) = \frac{1}{\lambda_1(t)}tr\left(F(t) - \frac{F(t)\psi(t)\psi^T(t)F(t)}{\delta(t)+\psi^T(t)F(t)\psi(t)}\right)$$

fixing the ratio $\delta(t) = \lambda_1(t)/\lambda_2(t) = const.$ Typical value: $\delta = 1$.

The updating of matrix F(t) is done using the U-D factorization for numerical robustness reasons. The details of this algorithm[7] are given in [13, Appendix B].

By taking $F(t) = \gamma I$, where I is the identity matrix, one gets a scalar adaptation gain. The equation (7) for updating the parameter vector becomes:

$$\hat{\theta}(t+1) = \hat{\theta}(t) + \gamma\psi(t)\frac{\nu^\circ(t+1)}{1+\gamma\psi^T(t)\psi(t)}. \quad (14)$$

When using scalar adaptation gain, for very small values of γ one can approximate the above equation by

$$\hat{\theta}(t+1) = \hat{\theta}(t) + \gamma\psi(t)\nu^\circ(t+1) \quad (15)$$

In the FULMS and FXLMS algorithms, since the adaptation gain is small and therefore the residual error will vary slowly, the quantity $\psi(t)\nu^\circ(t+1)$ is approximated by $\psi(t-1)\nu^\circ(t)$ leading to:

$$\hat{\theta}(t+1) = \hat{\theta}(t) + \gamma\psi(t-1)\nu^\circ(t) \quad (16)$$

Stability conditions

The a posteriori adaptation error ν is governed by an equation of the form:

$$\nu(t+1) = H_\nu(q^{-1})[\theta - \hat{\theta}]\phi(t) \quad (17)$$

[5] It is assumed that a reliable model identification is achieved and therefore the estimated model is assumed to be equal to the true model.

[6] Throughout the paper, n_X denotes the degree of the polynomial X.

[7] Routines for the implementation of the algorithm can be downloaded from `http://www.gipsa-lab.grenoble-inp.fr/~ioandore.landau/adaptivecontrol/`

where $\phi(t)$ is the observation (measurement) vector. This vector is always filtered by a filter L and (17) will take the form:

$$\nu(t+1) = H(q^{-1})[\theta - \hat{\theta}]\psi(t) \quad (18)$$

where

$$H(q^{-1}) = H_\nu(q^{-1})/L(q^-1) \quad (19)$$

Taking into account (18) for the a posteriori adaptation error and the equations for the PAA (7) through (11) one has the following condition for global asymptotic stability[8]:

$$H'(z^{-1}) = H(z^{-1}) - \frac{\lambda_2}{2}, \quad \max_t(\lambda_2(t)) \leq \lambda_2 < 2 \quad (20)$$

should be a strictly positive real (SPR) transfer function. For constant adaptation gains ($\lambda_2(t) = 0$) the stability condition becomes: $H(z^{-1})$ should be SPR. A key role in the stability of the various adaptation algorithms is played by the filter L operating on the observation vector ϕ. It helps to satisfy the "strictly positive real condition" for asymptotic stability.

6 Experimental Results

The objective of this section is to illustrate the performance which can be obtained with the techniques presented.

6.1 Adaptive feedback noise attenuation

6.1.1 Interference test

By interference, one refers to the effect occurring when two distinct waves with very close frequencies act together, creating periodic outbursts in the resulting wave magnitude. In this context two interferences are considered simultaneously and the frequencies are supposed unknown and time-varying.

The protocol is as follows: for 1 s, the system operates in open loop and without any disturbance in order to get a reference for the ambient noise. From 1 s to 10 s, the test bench works in open loop, in the presence of two pairs of sinusoidal noise disturbances located at 170 Hz and 170.5 Hz and 285 Hz and 285.5 Hz respectively. At 10 s, the loop is closed and the controller begins to counteract the disturbance effect. The frequencies of the four signals are then increased at 21 s by 10 Hz. The corresponding new values are 180 Hz and 180.5 Hz for the first pair and 295 Hz and 295.5 Hz for the second pair .

Figure 8 presents the results obtained with the adaptive feedback Youal-Kučera configuration. The number of adjustable parameters in the Q-filter is 4 ($n_Q = 3$) and an adaptation algorithm with *constant trace adaptation gain* is used. It can be seen that after a negligible transient, an excellent attenuation is obtained. The global attenuation obtained is 70.56 dB. Excellent levels of attenuation are also obtained once the disturbances frequencies move away by 10 Hz (global attenuation 67.65 dB), with a negligible adaptation transient

Figure 9 displays the evolution of the Q-parameters. From 0 s to 10 s, all the parameters have values equal to zero since the controller is not working yet. Once the loop is closed, the Q-parameters take almost instantly stable mean values. At 21 s, the change in frequencies leads to a quick adaptation towards the new values.

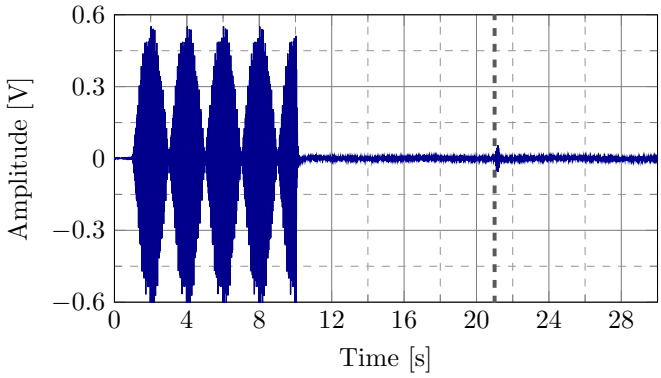

Figure 8: Acoustic interference attenuation using an adaptive controller. Noise frequencies:170+170.5 Hz, 285+285.5 Hz then 180+180.5 Hz, 295+295.5 Hz. Loop closed at 10 s.

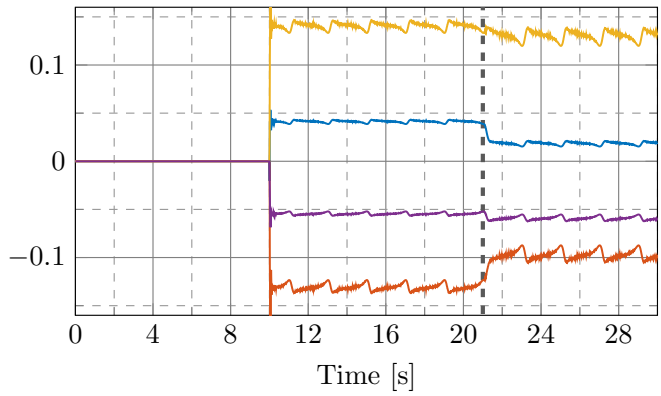

Figure 9: Parameters evolution for acoustic interference test using an adaptive controller.

6.1.2 Step changes in frequencies

In this experiment, step changes in the frequencies of a pair of tonal noise disturbances are considered, starting from their nominal values of 170 Hz and 285 Hz. The steps are of ±10 Hz and applied every 6.2 s. The system is operated in open loop from 0 s to 1 s.

The performance of the adaptive controller is illustrated in Fig. 10. The residual noise is close to the ambient noise. The adaptation transients are visible but very short. The evolution of the Q-parameters is shown in Fig. 11.

6.2 Adaptive feedforward noise attenuation

Figure 12 illustrates the evolution of the residual noise and of the attenuation over an horizon of 600 s for the Youla–Kučera feedforward compensator with an IIR Q filter with

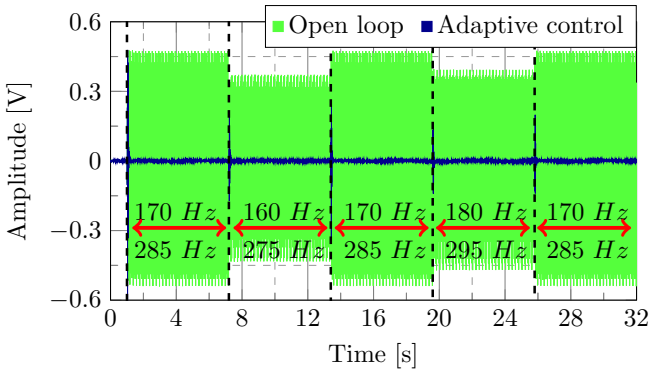

Figure 10: Step changes in frequencies using the adaptive controller. Residual noise in open loop (green) and in closed loop (blue)..

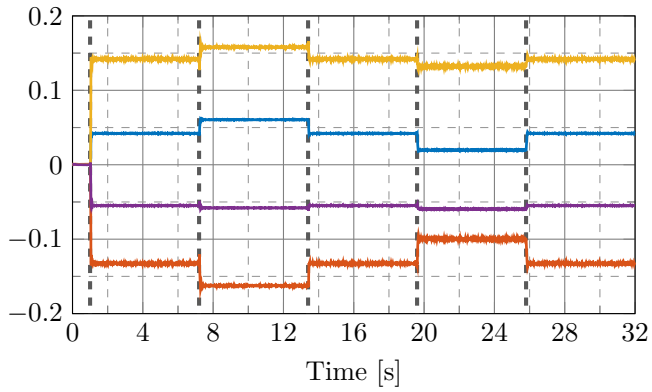

Figure 11: Evolution of the parameters of the adaptive controller in the presence of step changes in disturbances frequencies.

60 parameters (numerator : 30, denominator: 30) using the FUSBA algorithm [13] (matrix adaptation gain). Adaptation starts at t=15s. The disturbance has an almost flat spectrum between 70 and 270 Hz. Attenuation (also displayed on this figure) reaches almost the steady state value at 600s. The attenaution achieved is 35.72 dB. Figure 13 shows the PSD (power spectral density) for this configuration both in open loop and with the adptive feeforward compensator.

Figure 14 shows the adaptation capabilities of the IIRYK adaptive compensator with 30/30 parameters. One switch at t=180s from a flat disturbance between 170 to 270 Hz to a aflat disturbance between 70 to 170 Hz.

For the case when the length of the secondary path is larger than the length of the primary path (structure V3) experimental results can be found in [9].

7 Concluding remarks

A new methodology for adaptive active noise attenuation has emerged and extensive experimental results have been carried on to evaluate the performance. This new methodology can improve the performance of current solution for

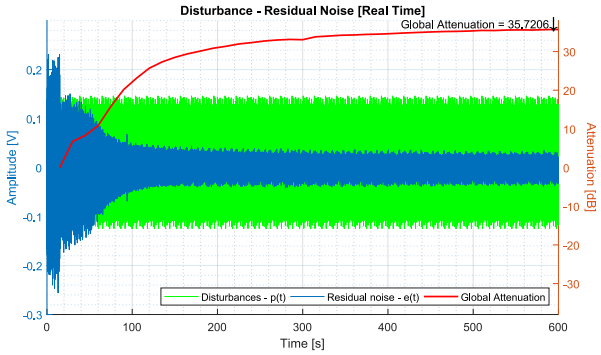

Figure 12: Residual noise using the IIRYK 30/30 adaptive compensators with FUSBA matrix adaptation (70-270 Hz disturbance, 600 s experiments).

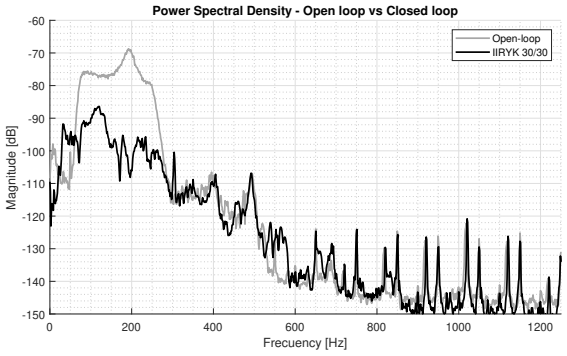

Figure 13: PSD of the IIRYK 30/30 adaptive compensators using FUSBA matrix adaptation (70-270 Hz disturbance, 600 s experiments).

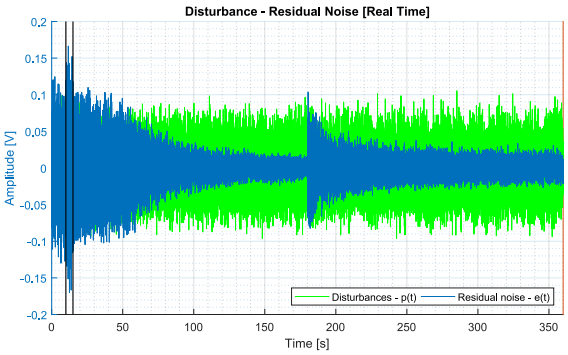

Figure 14: Residual noise of the IIRYK 30/30 adaptive feedforward compensator for a change of disturbance from 170 - 270 Hz to 70 - 170 Hz at 180 s.

active noise attenuation an opens the way for new applications.

References

[1] F. Ben Amara, P.T. Kabamba, and A.G. Ulsoy. Adaptive sinusoidal disturbance rejection in linear discrete-time systems - Part I: Theory. *Journal of Dynamic Systems Measurement and Control*, 121:648–654, 1999.

[2] F. Ben Amara, P.T. Kabamba, and A.G. Ulsoy. Adaptive sinusoidal disturbance rejection in linear discrete-time systems - Part II: Experiments. *Journal of Dynamic Systems Measurement and Control*, 121:655–659, 1999.

[3] S.J. Elliott and P.A. Nelson. Active noise control. *Noise / News International*, pages 75–98, June 1994.

[4] L.J. Eriksson. Development of the filtered-U LMS algorithm for active noise control. *J. of Acoustical Society of America*, 89(1):257–261, 1991.

[5] C.A. Jacobson, Jr. Johnson, C.R., D.C. McCormick, and W.A. Sethares. Stability of active noise control algorithms. *Signal Processing Letters, IEEE*, 8(3):74 –76, mar 2001.

[6] M.S. Kuo and D.R. Morgan. *Active noise control systems-Algorithms and DSP implementation*. Wiley, New York„ 1996.

[7] I. D. Landau, T.-B. Airimitoaie, and M. Alma. IIR Youla–Kučera parameterized adaptive feedforward compensators for active vibration control with mechanical coupling. *IEEE Transactions on Control System Technology*, 21(3):765–779, May 2013.

[8] I. D. Landau, R. Lozano, M. M'Saad, and A. Karimi. *Adaptive control*. Springer, London, 2nd edition, 2011.

[9] I. D. Landau, R. Melendez, T.B. Airimitoaie, and Luc Dugard. Robust and adaptive feedback noise attenuation in ducts. *Journal of Sound and Vibration*, 455, September 2019.

[10] I.D. Landau, R. Melendez, L. Dugard, and G. Buche. Why one should use youla-kucera parametrization in adaptive feedforward noise attenuation? In *Proceedings of the IEEE CDC Conference,Dec.2019, Nice, France*, 2019.

[11] I.D. Landau and G. Zito. *Digital control systems – Design, identification and implementation*. Springer, London, 2005.

[12] Ioan Doré Landau, Tudor-Bogdan Airimitoaie, and Marouane Alma. A Youla–Kučera parametrized adaptive feedforward compensator for active vibration control with mechanical coupling. *Automatica*, 48(9):2152 – 2158, 2012.

[13] Ioan Doré Landau, Tudor-Bogdan Airimitoaie, Abraham Castellanos Silva, and Aurelian Constantinescu. *Adaptive and Robust Active Vibration Control—Methodology and Tests*. Advances in Industrial Control. Springer Verlag, 2017.

[14] Ioan Dore Landau, Marouane Alma, and Tudor-Bogdan Airimitoaie. Adaptive feedforward compensation algorithms for active vibration control with mechanical coupling. *Automatica*, 47(10):2185 – 2196, 2011.

[15] Ioan Dore Landau, Raul Melendez, Luc Dugard, and Gabriel Buche. Robust and adaptive feedback noise attenuation in ducts. *IEEE Transactions on Control System Technology*, 27(2):872–879, March 2019.

[16] B. Widrow and S.D. Stearns. *Adaptive Signal Processing*. Prentice-Hall, Englewood Cliffs, New Jersey, 1985.

[17] J. Zeng and R.A. de Callafon. Recursive filter estimation for feedforward noise cancellation with acoustic coupling. *Journal of Sound and Vibration*, 291(3-5):1061 – 1079, 2006.